Computer Methods in Biomechanics and Biomedical Engineering, Vol. 3, pp. 321–334
Reprints available directly from the publisher
Photocopying permitted by license only

A Method for Numerical Simulation of Single Limb Ground Contact Events: Application to Heel-Toe Running

R. R. NEPTUNE[a,*], I. C. WRIGHT[a] and A. J. VAN DEN BOGERT[b]

[a]*Human Performance Laboratory, University of Calgary, Calgary, AB T2N 1N4;* [b]*Department of Biomedical Engineering, The Cleveland Clinic Foundation, Cleveland, OH 44195*

(Received 21 October 1998; In final form 23 December 1999)

The objective of this work was to develop a method to simulate single-limb ground contact events, which may be applied to study musculoskeletal injuries associated with such movements. To achieve this objective, a three-dimensional musculoskeletal model was developed consisting of the equations of motion for the musculoskeletal system, and models for the muscle force generation and ground contact elements. An optimization framework and a weighted least-squares objective function were presented that generated muscle stimulation patterns that optimally reproduced subject-specific movement data. Experimental data were collected from a single subject to provide initial conditions for the simulation and tracking data for the optimization.

As an example application, a simulation of the stance phase of running was generated. The results showed that the average difference between the simulation and subject's ground reaction force and joint angle data was less than two inter-trial standard deviations. Further, there was good agreement between the model's muscle excitation patterns and experimentally collected electromyography data. These results give confidence in the model to examine musculoskeletal loading during a variety of landing movements and to study the effects of various factors associated with injury.

Limitations were examined and areas of improvement for the model were presented.

Keywords: Optimization, musculoskeletal model, joint loading, injury, biomechanics, running

INTRODUCTION

Cumulative trauma disorders resulting from repetitive musculoskeletal loading account for 56% of all occupational injuries that currently affect 15% to 20% of all Americans (Melhorn, 1998). Even higher injury rates, including a variety of acute injuries, have been reported during recreational and competitive sport activities (e.g. Mummery *et al.*, 1998; Sandelin and Santavirta, 1991). Musculoskeletal

*Corresponding Author: Rehabilitation R & D Center (153), VA Palo Alto Health Care System, 3801 Miranda Avenue, Palo Alto, CA 94304 USA; E-mail: neptune@roses.stanford.edu

loads are influenced by factors such as the task being performed, anatomy, muscle coordination and equipment selection (e.g. footwear). For a given movement or task, muscle coordination and equipment selection are factors that can be altered within limitations to help reduce musculoskeletal loading. But it is not clear a priori how these factors will affect the loading because of the highly nonlinear dynamics and complex lower extremity movement kinematics. Changes in the movement caused by altered muscle forces and equipment selection result in changes in the muscle kinematics, and therefore, changes in the muscle forces. These circular dynamic interactions within the musculoskeletal system make these responses difficult to predict and interpret, and the effects are often counterintuitive. Understanding the dynamic interactions and the changes in joint loading associated with interventions is required for injury prevention and the design of safe and effective rehabilitation protocols. However, experimental studies have been limited in their ability to quantify joint loading during normal movement tasks due to technical and ethical limitations.

The effect of muscle properties, coordination changes and equipment selection on musculoskeletal loads can be examined systematically using theoretical musculoskeletal models. Such models require a sufficiently realistic mathematical representation of the skeletal dynamics, muscle forces and their dependence on length, velocity and activation, and contact forces with the environment. Two-dimensional (2D) sagittal plane models of human locomotion have been developed to simulate the various portions of gait (e.g. Davy and Audu, 1987; Pandy and Berme, 1988; Gerritsen *et al.*, 1998; Piazza and Delp, 1996) and the impact phase of running (Gerritsen *et al.*, 1995; Cole *et al.*, 1996). But the three-dimensional (3D) kinematic coupling within the lower extremity limits the ability of these 2D models to quantify joint loading accurately. Stacoff *et al.*, (1988) suggested that foot pronation is an important shock absorption mechanism during running and Nigg *et al.*, (1993) identified a kinematic link between pronation and internal rotation of the tibia which may generate undesired loads at the knee. Therefore, a 3D musculoskeletal model is needed to investigate locomotion and the associated joint loading.

Three-dimensional models of human locomotion have been developed (Gilchrist and Winter, 1997; Ju and Mansour, 1988; Pandy and Berme, 1989; Yamaguchi and Zajac, 1990), but these models were often simplified to reduce the computational demands. These models either restricted certain joint movements to the sagittal plane, did not include individual muscle actuators governed by activation dynamics and the force-length and velocity relationships, or they did not simulate the contact between the foot and ground at impact. Modeling the 3D movement at all joints is necessary to examine joint loading during non-sagittal plane movements (e.g. cutting and turning) and both the individual muscle forces and the ground contact force play an important role in determining the internal joint loads during dynamic movements. As computational speeds increase, the feasibility of producing full 3D simulations of human locomotion incorporating these necessary features is becoming more realistic.

Therefore, the objective of this project was to develop a 3D musculoskeletal model of the lower extremity with individual muscle actuators and ground contact elements and to generate a forward dynamic simulation of subject-specific movements that can be applied to studies of lower extremity loading during dynamic activities. Then, multiple subject-specific simulations may be performed and the results analyzed statistically, similar to the analysis of a group of human subjects. As an application of the model, heel-toe running was examined because it is associated with a high injury rate for both young (32%) and older (41%) age populations (Matheson *et al.*, 1989). This high injury rate yields an overall yearly incidence rate of running injuries between 37% and 56% (van Mechelen, 1992). Running is a highly dynamic movement with both a rapid impulsive loading phase at impact and a phase with large actively generated muscle forces that might contribute to the injury rate. Thus, a theoretical model of running may

provide insight into these injuries and is a useful test-case for the modeling methods that may be applied to other movements.

METHODS

To achieve the above objective, a forward dynamic simulation of heel-toe running was developed. This consisted of modeling the musculoskeletal system, muscle force generation and ground contact forces, identifying appropriate initial conditions, and using an optimization framework to identify the muscle controls to reproduce subject-specific movements. Experimental data were collected to provide initial conditions for the simulation (positions and velocities of the body segments at heel strike) and tracking data for the optimization of movement.

Musculoskeletal Model

A forward dynamic musculoskeletal model was developed using DADS 8.5 software (CADSI, Coralville, IA) and consisted of rigid segments representing the rear-foot, mid-foot, toes, talus, shank, patella, and thigh of the support leg, pelvis, and a rest-of-body segment (Figure 1). The pelvis had six degrees-of-freedom that permitted translation and rotation relative to ground. The rest-of-body segment was attached to the pelvis by a linear translational spring with three degrees-of-freedom and zero resting length. This rest-of-body represented the mass of the non-rigid components of the torso and all body segments that were not modeled: head, arms and the other leg. Eighty percent of the total mass of the head, arms and trunk was assigned to the rest-of-body segment with the remaining 20% being assigned to the pelvis (Cole *et al.*, 1997). The rest-of-body segment was treated as a point mass and the pelvis was given an inertia tensor that represented the entire upper body. The model was dimensioned to represent a male subject with a height of 180 cm and a mass of 75 kg. Musculoskeletal geometry was based on the work of Delp (1990) and segment masses and inertial properties were determined using regression equations (Clauser *et al.*, 1969; Chandler *et al.*, 1975).

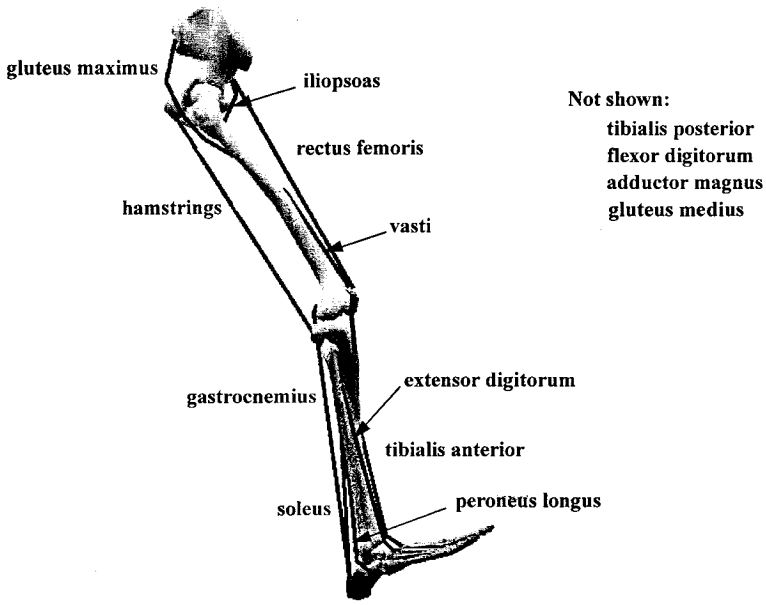

FIGURE 1 Musculoskeletal simulation model. The musculotendon actuator parameters are listed in Table I. Muscles are shown as straight lines for illustration purposes. The quadriceps and gluteus maximus muscles include non-fixed via points to provide appropriate lines-of-action through all joint excursions.

The joint models were based on existing literature. The hip joint had three degrees-of-freedom and was modeled as a spherical joint while the ankle had two degrees-of-freedom with rotations about the subtalar and talocrural joints (Inman, 1976). The tibiofemoral joint was modeled with three degrees-of-freedom with a moving centre of rotation for flexion-extension and appropriate passive stiffness for abduction-adduction and internal-external rotation (Markolf *et al.*, 1976). The patella was attached to the tibia by an inextensible patellar tendon and the origin of the patella was constrained to move along a prescribed trajectory relative to the femur Delp (1990), resulting in no additional degrees of freedom for the patellofemoral joint. The foot consisted of three segments: rear-foot, mid-foot and toes. Flexion/extension and internal/external rotation were allowed between the rear-mid and mid-foot, and flexion/extension was allowed between the mid-foot and toes for a total of three degrees-of-freedom. Therefore, the model had a total of 20 degrees-of-freedom. Passive stiffnesses were applied at these joints so that realistic displacements were achieved during mid-stance.

TABLE I Musculotendon actuator parameters. The muscles included in the model were the gluteus maximus (GMAX), iliopsoas (PSOAS), adductor magnus (ADDMAG), gluteus medius (GMED), hamstrings (HAMS), rectus femoris (RF), vasti lateralis, intermedius, medialis longus and medialis obliques (VAS), gastrocnemius (GAS), peroneus longus (PER), soleus (SOL), tibialis posterior (TIBPOST), tibialis anterior (TA), extensor digitorum longus (EXTDIG) and flexor digitorum longus (FLEXDIG). The four vasti muscles all received the same excitation signal

Muscle	Peak Isometric Force (N)	Optimal Fiber Length (m)	W	Tendon Slack Length (m)
GMAX	1752	0.144	0.63	0.126
PSOAS	800	0.099	1.3	0.090
ADDMAG	1578	0.138	0.56	0.110
GMED	3005	0.080	0.80	0.053
HAMS	1769	0.120	1.2	0.319
RF	1560	0.084	1.44	0.346
VAS				
lateralis	1871	0.084	0.63	0.157
intermedius	1365	0.087	0.63	0.136
med longus	647	0.089	0.63	0.126
med obliques	647	0.089	0.63	0.126
GAS	3210	0.043	0.89	0.408
PER	1015	0.048	0.56	0.345
SOL	5660	0.027	1.03	0.268
TIBPOST	1270	0.030	0.56	0.310
TA	2000	0.098	0.44	0.223
EXTDIG	2000	0.101	0.56	0.345
FLEXDIG	1260	0.034	0.56	0.400

Muscle Force Model

Fourteen functionally independent muscle groups were used to drive the model (Table I). Each muscle had an origin and insertion point fixed relative to model segments. Several muscles had additional fixed via points to describe the muscle paths more accurately (Delp, 1990). Some muscles were given additional non-fixed points that represented wrapping of the muscle paths around underlying bones and muscles as the segments moved. The vasti muscle group was constrained to pass on the anterior side of a line pointing laterally based on the via points of Delp (1990). The gluteus was constrained to pass posteriorly around a cylinder (5 cm radius) located at the hip joint centre to prevent the muscle's line-of-action from passing through the hip joint centre. The 5 cm radius was chosen to produce a moment arm similar to Delp (1990) when the model was in its anatomical position. The wrapping points were generated by examining the path of the muscle at each time step. If the muscle path was directed on the wrong side of the line or cylinder, then the tangent points from the cylinder to the via points either proximal or distal to the line or cylinder were calculated using the algorithms of van der Helm (1991) and these points were used as additional via points at that time step.

Force production in muscles was represented by three-component Hill models (Figure 2), consisting of a contractile element (CE), series elastic element (SEE), and parallel elastic element (PEE). Maximum isometric CE force, optimal muscle fibre (CE) length, and SEE slack length values were taken from Delp (1990). The contractile element force-length relationship was modeled as a parabolic function (Soest and Bobbert, 1993). The values for muscle parameter W, the maximum active length change relative to the optimal fibre length were taken from Gerritsen and Bogert (1995) (Table I).

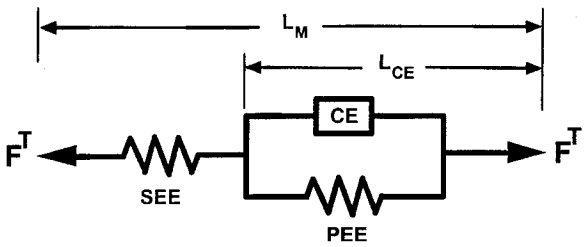

FIGURE 2 Musculotendon model. The musculotendon force (F^T) is a function of the contractile element (CE), series elastic element (SEE) and parallel elastic element (PEE). F^T is computed and applied to the associated origin, insertion and via points on each segment.

The contractile element force-velocity relationship was modeled using hyperbolic functions and scaling methods from Soest and Bobbert (1993). The normalized properties of the parallel elastic and series elastic elements were also taken from Soest and Bobbert (1993). This three-component Hill model is mathematically represented by a single first-order ordinary differential equation (ODE) with state variable L_{CE}, the instantaneous length of the contractile element:

$$\dot{L}_{CE} = f(L_{CE}, L_M, a) \tag{1}$$

The muscle activation (a) was coupled to the neural excitation (u) through another first-order ODE (He *et al.*, 1991), with activation and deactivation time constants of 10 and 30 ms, respectively (Winters and Stark, 1988) as:

$$\dot{a} = (u - a) \cdot (c_1 u + c_2) \tag{2}$$

where c_1 and c_2 are functions of the activation and deactivation time constants with $c_1 = \tau_{act}^{-1} - \tau_{deact}^{-1}$ and $c_2 = \tau_{deact}^{-1}$. Each muscle therefore adds two ODE's and two state variables (L_{CE} and a) to the model.

For running, the neural excitation pattern for each muscle was modeled as a single block pattern defined by three parameters: onset, duration, and magnitude. The onset of muscle excitation was allowed up to 150 ms before touchdown as observed in collected EMG data. Based on collected EMG data, TA was assigned a 2-burst pattern with the following three parameters: magnitude, offset and duration of the silent phase. With fourteen muscles, 42 parameters were therefore required to describe the complete muscle coordination pattern.

Ground Contact Model

The contact between the foot and the ground was modeled by 66 discrete independent viscoelastic elements, each attached to one of the three foot segments in locations that describe the 3-D exterior surface of a shoe when the foot joints are in a neutral position. Each element permitted deformation perpendicular to the floor and represented the

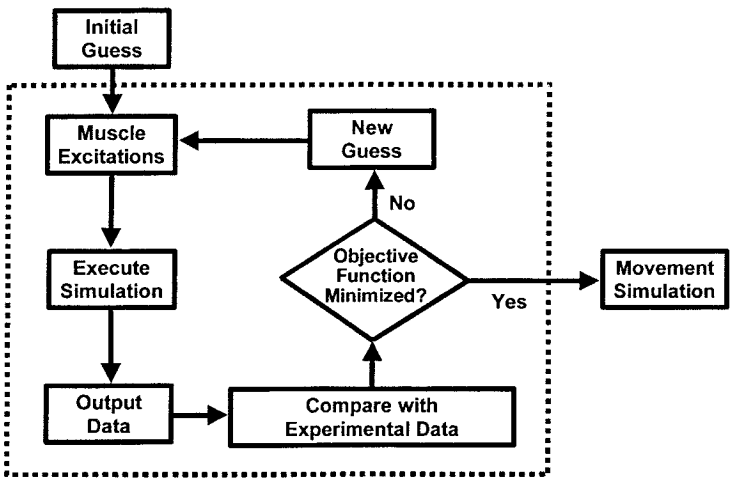

FIGURE 3 Schematic diagram of the optimization framework.

mechanical properties of the shoe sole and underlying soft tissue. The vertical force of each element was calculated as:

$$F_{contact}(i) = \max \begin{bmatrix} 0 \\ area(i) \cdot (c_1 \cdot dz(i)^{c_2} \\ \quad + c_3 \cdot dz(i)^{c_4} \cdot d\dot{z}(i)^{c_5}) \end{bmatrix} \quad (3)$$

where

$F_{contact}(i)$ = vertical force of element i (units in N)

$c1, c2, c3,$ $c4$ and $c5$ = shoe-specific parameters

$dz(i)$ = vertical deformation of element i (units in m)

$d\dot{z}(i)$ = vertical velocity of element i (units in m/s)

$area(i)$ = relative element area scaling factor

Shoe specific parameters were determined for a soft running shoe (Table II). A pendulum impact test was simulated with the ground contact model and parameters were determined that reproduced experimentally collected pendulum impact force-deformation curves (Aerts and De Clercq, 1993). The relative area scaling factor scaled the mechanical properties of each element relative to the mechanical properties of the area used in the pendulum impact test. Each element was assumed square and an additional area outside each square equaled a constant w (0.01 m) multiplied by the length of the perimeter deformed during contact. Therefore, $area(i)$ was calculated as:

$$area(i) = \frac{A(i) + 4w\sqrt{A(i)}}{A_{pend} + w\sqrt{\pi A_{pend}}} \quad (4)$$

TABLE II Shoe Specific Parameters for a Soft running Shoe Derived from Aerts and De Clercq (1993)

Shoe Parameter	Value
C1	60,00,000
C2	2.20
C3	−16,000
C4	0.80
C5	1.50
C6	3,000
C7	0.7

where

$A(i)$ = area of element i

A_{pend} = area of pendulum (32.2 cm^2, Aerts and De Clercq, 1993)

Anterior-posterior and medial-lateral forces at each element were modeled as a Coulomb friction force resisting slipping of the foot relative to the ground (Cole *et al.*, 1996) as:

$$F_{fric}(i) = area(i) \cdot c_6 \cdot d\dot{x}(i) \quad if\ |F_{fric}(i)| \leq c_7 \cdot F_{contact}(i)$$

$$F_{fric}(i) = -c_7 \cdot F_{contact}(i) \cdot sign(d\dot{x}(i)) \quad if\ |F_{fric}(i)| > c_7 \cdot F_{contact}(i) \quad (5)$$

where

$F_{fric}(i)$ = horizontal frictional force (units in N)

$d\dot{x}(i)$ = horizontal velocity of element i (units in m/s)

C_6 = viscous damping coefficient for low sliding velocities

C_7 = friction coefficient of the shoe

For true Coulomb friction, parameter C_6 should be infinity but this is not possible for numerical reasons. In the approximation (5), viscous behaviour is limited to sliding velocities less than $C_7/C_6^* F_{contact}$, which is sufficiently close to zero for practical purposes.

Initial Conditions

Initial kinematic conditions for the simulations were derived from measured experimental kinematic data. For one subject, 10 running trials were performed (described below). A standing neutral trial was used to define a limb segment fixed coordinate system for the pelvis, thigh, shank and rear-foot. The orientation of each limb segment plus the position of the shank segment relative to the laboratory were determined from the marker displacement data using a singular value decomposition method (Soderkvist and Wedin, 1993). Inverse kinematic analysis was performed on these data to determine the model configuration, in terms of the

kinematic degrees of freedom, that best matched these segment positions. The kinematic data were fit with a quintic spline (GCVSPL, Woltring, 1986) and sampled at 1000 Hz. Then a finite difference method was used to determine the first derivative of each independent kinematic variable at touchdown. The segment positions, orientations and first derivatives of these variables at touchdown were averaged across the 10 trials and used as the initial conditions for the simulation. The initial position of the rest-of-body mass was chosen to produce zero force in its elastic attachment to the pelvis since both are in free fall before touchdown.

The individual muscle excitations were pre-integrated using Equation (2) over the 150 ms duration before touchdown to identify the appropriate initial muscle activation levels. The tendon length was set to its slack length and the initial muscle CE length was determined by computing the difference between the initial total musculotendon length and the tendon slack length.

Optimization Method

A simulation of subject specific running mechanics was produced by searching for the muscle excitation patterns that minimized the difference between simulated and measured segment orientations and external ground reaction force profiles (Equation 6), for the same individual used to determine the initial conditions, using a simulated annealing optimization algorithm (Goffe *et al.*, 1994) (Figure 3). Data for the rest-of-body stiffness were not found in the literature, therefore the stiffness was included as a parameter to be optimized and was allowed to vary between 0 and 40 kN/m. This yielded a total of 43 variables (14 muscle excitation patterns and one stiffness) to be optimized. The objective function to be minimized was defined as:

$$J(p) = \sum_{j=1}^{m} \sum_{i=1}^{n} \frac{(Y_{ij} - \hat{Y}_{ij})^2}{SD_j^2} \qquad (6)$$

where

Y_{ij} = measurement of variable j at time step i

$\hat{Y}_{ij}$ = simulation data corresponding to Y_{ij}

SD_j^2 = average inter-trial variability of variable j

p = $(p_1 \ldots p_{43})$, the parameters describing the neural excitation patterns and rest-of-body mass stiffness

This form of the objective function (Equation 6) was used in a previous pedaling simulation study (Neptune and Hull, 1998) and effectively produced simulations that reproduced experimental data. The specific quantities evaluated in Equation (6) were the four Euler parameters describing the global attitude matrix of the rear-foot, shank and thigh, and the three (x,y,z) components of the ground reaction force, resulting in a total of m = 15 variables included in the objective function (Equation 5). The optimization was terminated when the cost function did not decrease the objective function by 1% within 500 function calls.

Experimental Data

To provide initial conditions for the simulation (positions and velocities of the body segments at touchdown) and tracking data for the optimization algorithm, experimental data were collected from one healthy male subject (height = 186 cm; weight = 82.0, age = 45.0 years) during heel-toe running. The subject volunteered to participate in the study and informed consent was obtained before the data collection.

The subject performed ten trials of heel-toe running at 4.0 ± 0.4 m/s while kinematic and ground reaction force data were collected. Three retro-reflective markers were attached to the subject's right shoe (lateral head of the fifth metatarsal, posterior heel, superior lateral aspect of the navicular), shank (head of fibula, anterior mid-shaft of tibia, and distal fibula just proximal to the lateral maleolus), thigh (greater trochanter, anterior mid-thigh, lateral femoral epicondyle) and pelvis (left and right anterior superior illiac spines, and right posterior superior illiac spine). A high-speed video system

(Motion Analysis Corp., Santa Rosa CA) was used to track the three-dimensional motion of the markers at 240 frames per second. The marker data were used to reconstruct the position and orientation of each body segment (Soderkvist and Wedin, 1993). The attitude matrices for each segment were converted to Euler parameters to describe the segment orientations relative to the global coordinate system. From the limb segment orientations, hip and knee angles were determined using the joint-coordinate system of Grood and Suntay (1983) and the subtalar and talocural joint angles were determined using the joint-coordinate system of Inman (1976) which corresponds to the orientation of the hinge axes in the model (Delp, 1990).

Ground reaction force data were collected simultaneously with the kinematic data at 2400 Hz using a force platform (Kistler Instumente AG, Winterthur, Switzerland). The time of heel strike was determined when the vertical ground reaction force first exceeded 20 N and toe-off was indicated when the vertical ground reaction force fell below 20 N. All trials were normalized to the duration from heel strike to toe-off, and the forces and joint angles were resampled at intervals of 1/100 of the stance duration. The forces were then normalized to body weight.

Surface EMG data were simultaneously collected from 10 lower extremity muscles at 2400 Hz to provide data for comparison with the optimized muscle stimulation patterns of the model. Bipolar electrodes (Biovision, Wehrheim, Germany) were placed on the soleus, medial gastrocnemius, peroneus longus, tibialis anterior, vastus medialis, vastus lateralis, rectus femoris, biceps femoris, adductor magnus and the gluteus maximus based on the work of Delagi *et al.*, (1979). The skin at each electrode site was shaved and cleaned with alcohol. The raw EMG signal was bandpass filtered with cut-off frequencies of 30 and 1000 Hz with a common mode rejection ratio of 120 dB. During post processing, the EMG data were rectified and smoothed using a 40 ms moving average window and normalized to the maximum value achieved during the stance phase.

Model Validation

The following criteria were used to validate the model:

1. All 15 simulated variables that were included in the cost function should, after optimization, be within two inter-trial standard deviations of the corresponding subject data. This means that there is a 95% probability that the simulation belongs to the same statistical distribution that generated the experimental data.
2. Optimized muscle excitation patterns should correspond qualitatively to EMG measurements.
3. The mechanical response of the model to perturbations should be compared to the response of human subjects.

The present paper will only report on criteria 1 and 2. Perturbation experiments with the model were reported elsewhere (Wright *et al.*, 1999).

RESULTS

Typical execution time to simulate the 0.248 s heel-toe running required 460 seconds CPU time on a Silicon Graphics Indigo 2 workstation with a 195 MHz R10000 processor (Silicon Graphics, Inc., Mountain View, CA). The optimization algorithm was effective in reducing the objective function value and converged within 5000 function calls.

The optimization was able to determine the muscle controls (excitation onset, offset and magnitude) to reproduce the salient features of the experimentally collected data (Figures 4–6). The major joint angles and ground reaction forces were almost always within 2 SD of the subject's data. Deviations from the experimental data occurred in the non-sagittal plane angles in the knee joint (Figure 5). Although not presented, similar deviations occurred at the hip joint since muscles did not actively control the pelvis.

Muscle stimulation patterns compared well with the collected EMG data (Figure 6). Differences were apparent in the onset timing of adductor magnus, rectus femoris and gastrocnemius while there was

close agreement in the muscle stimulation offset except for rectus femoris, vasti and soleus.

Sagittal plane hip, knee and ankle joint loads are presented in Figure 7. The compressive loads in all three joints exceeded eight times body-weight with peak values occurring during the active loading phase at mid-stance. Shear forces were largest at the hip joint and systematically decreased at the knee and ankle joints, respectively.

DISCUSSION

The objective of this work was to develop a 3D model of the lower extremity with individual muscle actuators and ground contact elements to examine musculoskeletal loading during subject-specific impact events. To this end, we generated a forward dynamic simulation of running that reproduced experimental data from a single subject. Before the utility of the model is discussed further, the validity of the running simulations should be addressed. In the present study, the average difference between the model and human subject's ground reaction force and joint angle data was less than two inter-trial standard deviations (Figures 4 and 5). Although larger deviations occurred in the knee nonsagittal plane angles from the experimental data, these angles were within the errors expected in experimental kinematic data due to the use of external markers (Reinschmidt *et al.*, 1997). The largest discrepancy occurred in the hip adduction/abduction because we did not control the rest-of-body segment with active muscle forces.

There was good qualitative agreement between the muscle stimulation patterns and the subject's EMG data (Figure 6), especially for the larger muscles. This is encouraging, since it shows that the model functioned similar to the human body for this task, and is therefore a useful research tool. However, there are also striking differences that indicate the model is apparently able to reproduce the subject's external kinematics and forces with different muscle stimulation patterns. This may have been caused by the relative insensitivity of the cost

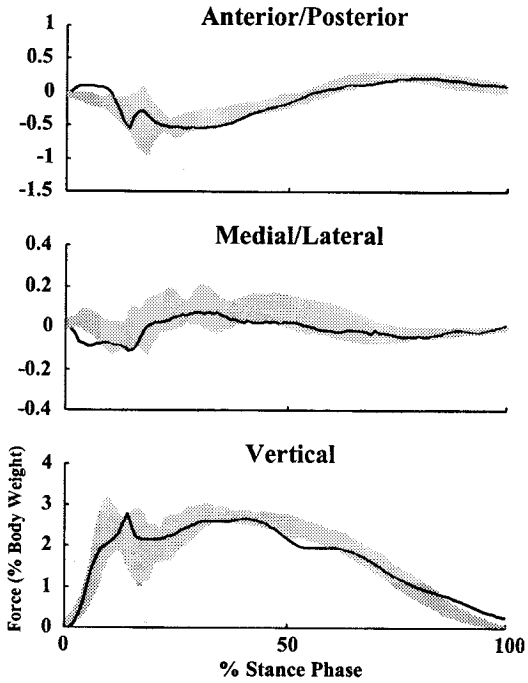

FIGURE 4 Ground reaction force comparisons between the subject's mean data and the simulation data. Gray area represents ±2 standard deviations.

function to certain changes in the 42 muscle stimulation parameters, which results in large changes in muscle stimulation pattern for relatively small reductions in cost function. This could be prevented by incorporating EMG timing variables into the cost function (Neptune and Hull, 1998). Alternatively, a better-defined minimum of the cost function could be obtained by reducing the number of parameters, for instance by grouping muscles together into units with similar stimulation patterns. The fact that external kinematics and forces could be reproduced to within two inter-trial standard deviations means that the model's running mechanics was indistinguishable from an arbitrary movement trial of the corresponding human subject.

The ability of the model to simulate the response to interventions during the landing phase of running was investigated in a separate study (Wright *et al.*, 1999). The model was subjected to ground surface perturbations and the resulting ground reaction forces and joint angles were compared to subject data during the same perturbations. The model

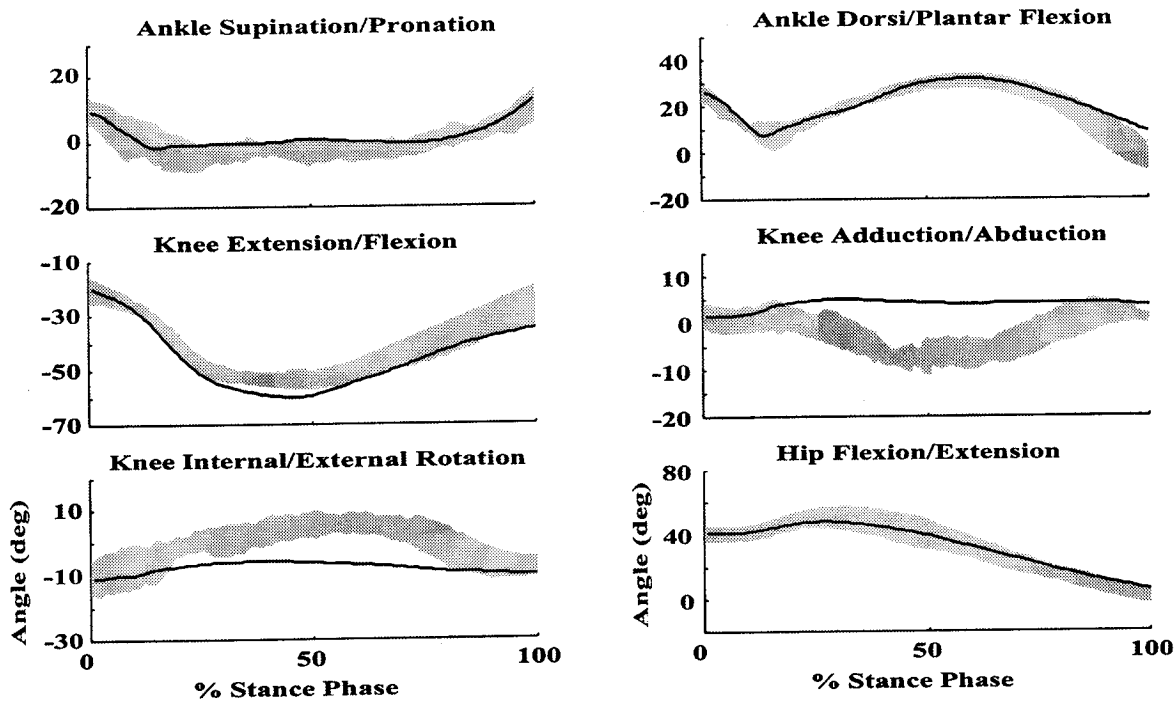

FIGURE 5 Joint angle comparisons between the subject's mean data and the simulation data. Gray area represents ±2 standard deviations.

responded similarly to the subjects indicating that the model contained all biomechanical mechanisms necessary to predict the subject responses. Specifically, these responses are dependent on joint stiffness, and therefore on antagonistic co-activation that is not well resolved by the optimization based on external kinematics and forces, as described above. These results, combined with the agreement in force, kinematics, and EMG of the unperturbed movement, provide confidence that the model may be used for experiments that cannot be performed on human subjects.

Previous studies have examined parameter sensitivities in similar musculoskeletal models and found the models to be robust. These parameters included maximum isometric force (Neptune and Hull, 1998), activation and deactivation time constants (Piazza and Delp, 1996; Raasch *et al.*, 1997) and subject height (Schutte *et al.*, 1993). The sensitivity of the ground reaction force to variations in the shoe parameters was also previously investigated in Wright *et al.*, (1998). The results showed that the ground reaction force was insensitive to shoe stiffness variations. Although those authors did not directly examine joint loading, the kinematics of the movement and ground reaction forces were similar across parameter variations, and therefore, joint loading would be insensitive to parameter variations as well.

One limitation of the model is a lack of a control system similar to the human central nervous system that includes continuous sensory feedback to modulate the excitation patterns. Such a system would be important to study upright balance and control questions and could be incorporated into the model (e.g. Gerritsen, 1998). The feed-forward control muscle stimulation used in the present study allows full control over muscle stimulation, and therefore, makes it possible to study the effect of mechanical interventions and muscle coordination on joint loading without the confounding effect of subject adaptation (e.g. Ferris *et al.*, 1999). It should be noted however, that for some applications it may be necessary

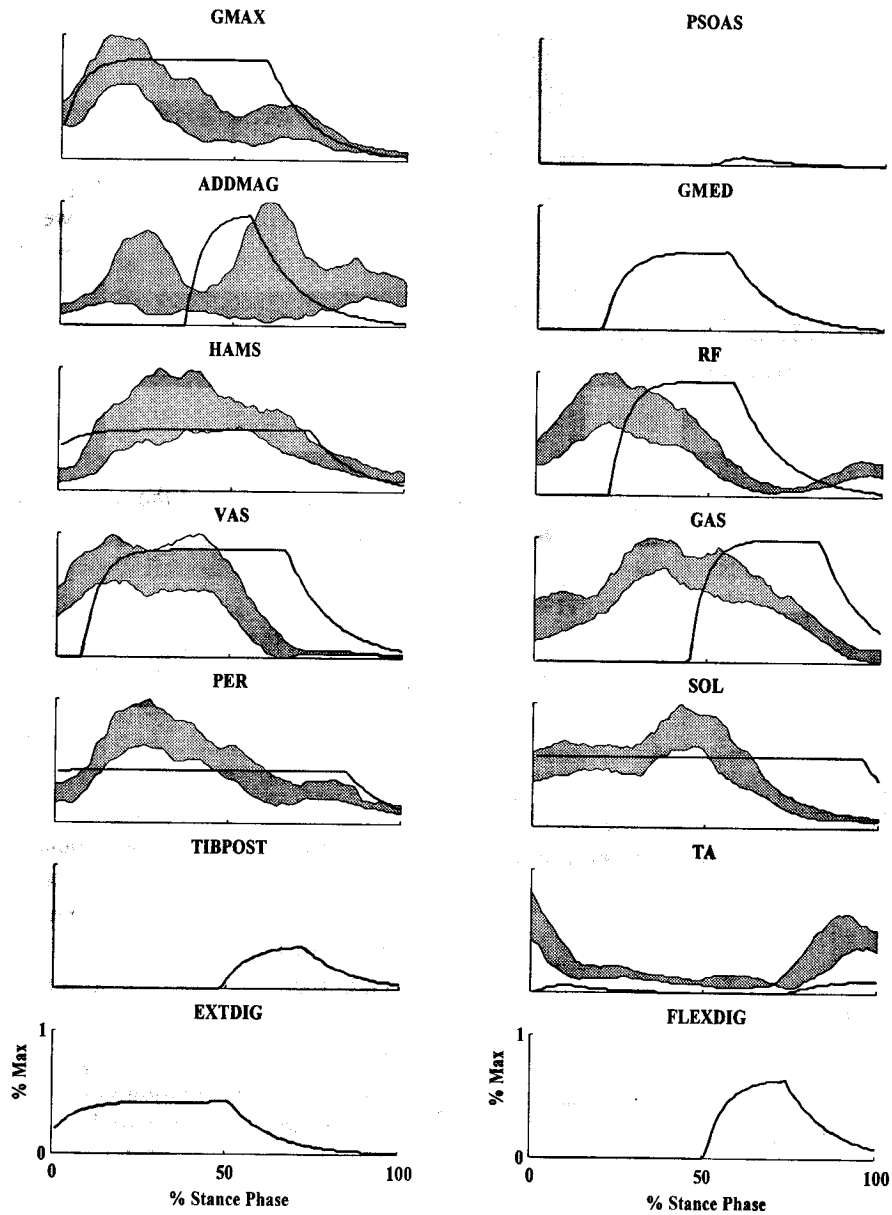

FIGURE 6 Muscle excitation timing comparison between the subject's mean data and the simulation data. Gray area represents ±1 standard deviations.

to model reflexes that play a role during certain movements.

The simulated joint loading patterns were similar at the hip, knee and ankle (Figure 7). Peak values occurred at mid stance during the active loading phase when active muscle forces are combined with the inertial loads and gravity to compress the joints. The forces at the hip joint may be compared to the direct measurements of Bergmann *et al.*, (1993) who reported a peak load of five times body weight during slow running (2.2 m/s), while our simulation ran at 4.0 m/s and generated a peak force of eight times body weight. The simulation results may represent the upper limit in joint loading since the model did not explicitly consider co-contraction in the objective function, other than as a method to produce

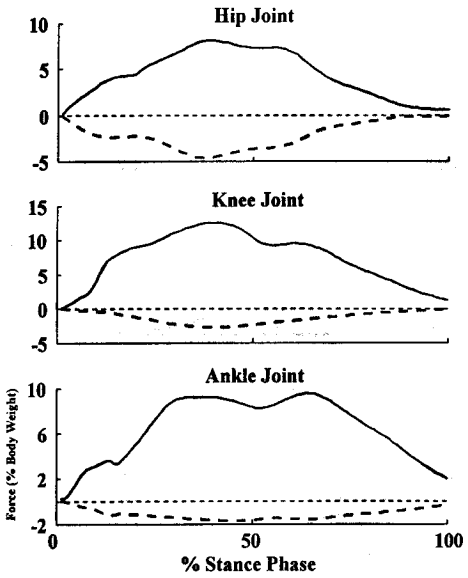

FIGURE 7 Compressive (solid line) and shear (dashed line) joint loading patterns for the hip, knee and ankle joint in the sagittal plane. Forces are expressed in the pelvis, femur and talus body-fixed coordinate systems, respectively. Negative shear is directed posteriorly.

the desired dynamic limb stiffness. Results from inverse dynamic analysis typically represent a lower limit because optimization criteria are used that discourage co-contraction. Aside from these limitations, modeling and simulation provides a powerful tool to examine mechanisms behind joint loading and the effectiveness of various interventions (e.g. shoe orthoses) to reduce joint loading. An application of the present model to study treatments for patellofemoral joint pain is presented elsewhere (Neptune *et al.*, 1999). The optimization framework described in this study allowed us to develop simulations based on the movement and external loading patterns of a specific individual. This is important for the study of a nonlinear system such as a runner during the stance phase. It has been shown, both in human experiments (Nigg *et al.*, 1987) and in simulations (Wright *et al.*, 1998) that results of footwear modifications are sensitive to the running style of the individual. Our subject-specific movement optimization approach allows simulations of multiple individuals to be developed, and therefore, allows statistical analysis and prevents incorrect generalizations of simulation results to the general population. For these complex dynamic systems, results from a single model cannot be generalized (Wright *et al.*, 1998). In the present study, no attempt was made to adapt the model to subject-specific anatomy and/or inertial properties. This will be important for certain applications of the model and requires further development of the methodology. However, it should be noted that introducing subject-specific anatomy in addition to subject-specific movements would make it impossible to attribute differences between subjects to either the movement or to the anatomy. Certain components in the model require improvement. A "rest-of-body" mass was included in the model to represent the movement of soft tissue relative to the rigid pelvis and the other limb segments not included in the model. The attachment of this mass to the pelvis was modeled as a linear spring. The stiffness was an unknown and included as a parameter to be optimized. This linear approximation of a very nonlinear system makes the stiffness and mass of this element dependent on frequency and amplitude and this should be carefully considered when simulating other movements. For the present study, this rest-of-body mass provided an effective way to produce appropriate ground reaction forces and movement kinematics that were necessary to examine joint loading during running. In the future, modeling of other limb segments may be necessary depending on the questions of interest.

Identifying appropriate passive joint stiffnesses for the model was also difficult with little information available in the literature. Currently, the passive stiffnesses were mostly based on cadaver data and may not be indicative of dynamic joint stiffness *in vivo* and may vary considerably between individuals. We recommend that passive joint torques should be carefully modeled for movements and injuries that involve large joint rotations (e.g. ankle sprains). Subject-specific models may be required and the addition of discrete ligament structures, rather than passive joint torques, would allow the examination of ligament forces during dynamic loading conditions which would have important implications in designing rehabilitative protocols after reconstructive surgery. During a normal running movement,

as shown in the present simulation example, passive joint torques are extremely low and do not influence the results.

Further improvements can be made to the excitation patterns. The current optimization framework assumed that the muscle excitation patterns were single burst block patterns except for the TA that had a 2-burst pattern. These patterns were chosen due to the computational demand of additional parameters necessary to describe more complex patterns (Anderson *et al.*, 1995). Allowing arbitrary excitation patterns would further reduce the tracking errors and may result in a closer agreement with the EMG data. However, it may also result in less agreement with EMG data since there will be more opportunity for the optimization algorithm to make changes in stimulation patterns in order to achieve small reductions in the cost function. These issues need to be explored further.

Future Studies

Despite the limitations discussed above, the musculoskeletal model and simulation developed met the criteria set out in the Introduction. The model can be used to examine internal joint loading during impact-type events. The model will allow us to examine the mechanics behind joint loading to provide insight into the mechanics of overuse injuries. The strength of using simulations is that it allows us to perform a set of experiments on subject specific simulations and to apply interventions and quantify individual muscle forces and internal joint loading. Future studies may also include the optimization of shoe and orthotic designs and knee and ankle bracing systems to reduce joint loading.

The same methodological framework may also be applied to study movements where acute injuries occur when exposed to certain external conditions. Currently, the model is being applied to analyze ankle sprain injuries due to landing on uneven surfaces (Wright *et al.*, 2000). Simulation is an excellent tool to experiment with such movements without risk to human or animal subjects. Questions related to locomotor performance, rather than loading of tissues, may also be studied. Such questions may range from the design of prostheses, control systems for functional electrical stimulation, or predicting the effect of tendon transfer surgery in patients with musculoskeletal disorders. The numerical methods described in this paper provide the framework to develop subject-specific movement simulations for such studies.

Acknowledgments

The authors are grateful to The Natural Sciences and Engineering Research Council of Canada, The Whitaker Foundation and Adidas for providing funding for this research.

References

Aerts, P. and De Clercq, D. (1993). Deformation characteristics of the heel region of the shod foot during a simulated heel strike: the effect of varying midsole hardness. *J Sports Sci*, **11**, 449–461.

Anderson, F. C., Ziegler, J. M., Pandy, M. G. and Whalen, R. T. (1995). Application of high-performance computing to numerical simulation of human movement. *J Biomech Eng*, **117**, 155–157.

Chandler, R. F., Clauser, C. E., McConville, J. T., Reynolds, H. M. and Young, J. W. (1975). Investigation of inertial properties of the human body. Wright Patterson Air Force Base, Ohio (AMRL-TR-75-137).

Clauser, C. E., McConville, J. T. and Young, J. W. (1969). Weight, volume and center of mass of segments of the body. Wright Patterson Air Force Base, Ohio (AMRL-TR-69-70).

Cole, G. K., Nigg, B. M., Bogert, A. J. van den and Gerritsen, K. G. M. (1996). Lower extremity joint loading during impact in running. *Clin Biomech*, **11**, 181–193.

Davy, D. T. and Audu, M. L. (1987). A dynamic optimization technique for predicting muscle forces in the swing phase of gait. *J Biomech*, **20**, 187–201.

Delagi, E. F., Perotto, A., Iazzetti, J. and Morrison, D. (1979). Anatomic Guide for the Electromyographer: the Limbs. Springfield, Il: Charles C. Thomas.

Delp, S. L. (1990). A computer graphics system to analyze and design musculoskeletal reconstructions of the lower limb. Ph.D. Dissertation, Stanford University, Stanford, CA.

Ferris, D. P., Liang, K. L. and Farley, C. T. (1999). Runners adjust leg stiffness for their first step on a new running surface. *J Biomech*, **32**(8), 787–794.

Gerritsen, K. G. M. and Bogert, A. J. van den. (1995). Force-length parameters of lower extremity muscles derived from maximal isometric tests. Proceedings of the XIXth Annual Meeting of the American Society of Biomechanics, Stanford, CA.

Gerritsen, K. G., Bogert, A. J. van den and Nigg, B. M. (1995). Direct dynamics simulation of the impact phase in heel-toe running. *J Biomech*, **28**, 661–668.

Gerritsen, K. G., Bogert, A. J. van den., Hulliger, M. and Zernicke, R. F. (1998). Intrinsic muscle properties facilitate locomotor control — a computer simulation study. *Motor Control*, **2**, 206–220.

Gerritsen, K. G. M. (1997). Computer Simulation of FES-Assisted Locomotion. Ph.D. Dissertation, University of Cagary, Calgary, AB, Canada.

Gilchrist, L. A. and Winter, D. A. (1997). A multisegment computer simulation of normal human gait. *IEEE Trans Rehabil Eng*, **5**, 290–299.

Goffe, W. L., Ferrier, G. D. and Rogers, J. (1994). Global optimization of statistical functions with simulated annealing. *Journal of Econometrics*, **60**, 65–99.

Grood, E. S. and Suntay, W. J. (1983). A joint coordinate system for the clinical description of three-dimensional motions: application to the knee. *J Biomech Eng*, **105**, 136–144.

He, J., Levine, W. S. and Loeb, G. E. (1991). Feedback gains for correcting small perturbations to standing posture. *IEEE Trans Autom Control*, **36**, 322–332.

Inman, V. T. (1976). The joints of the ankle. Baltimore: Williams and Wilkins.

Ju, M. S. and Mansour, J. M. (1988). Simulation of the double limb support phase of human gait. *J Biomech Eng*, **110**, 223–229.

Markolf, K. L., Mensch, J. S. and Amstutz, H. C. (1976). Stiffness and laxity of the knee — the contributions of the supporting structures. A quantitative in vitro study. *J Bone Joint Surg*, [Am] **58**, 583–594.

Matheson, G. O., Macintyre, J. G., Taunton, J. E., Clement, D. B. and Lloyd-Smith, R. (1989). Musculoskeletal injuries associated with physical activity in older adults. *Med Sci Sports Exerc*, **21**, 379–385.

Melhorn, J. M. (1998). Cumulative trauma disorders and repetitive strain injuries. The future. *Clin Orthop*, 107–126.

Mummery, W. K., Spence, J. C., Vincenten, J. A. and Voaklander, D. C. (1998). A descriptive epidemiology of sport and recreation injuries in a population-based sample: results from the Alberta Sport and Recreation Injury Survey (ASRIS). *Can J Public Health*, **89**, 53–56.

Neptune, R. R. and Hull, M. L. (1998). Evaluation of performance criteria for simulation of submaximal steady-state cycling using a forward dynamic model. *J Biomech Eng*, **120**, 334–341.

Neptune, R. R., Wright, I. C. and van den Bogert, A. J. (1999). The influence of orthotic devices and vastus medialis strength and timing on patellofemoral loads during running. *Clin Biomech*, Accepted.

Nigg, B. M., Cole, G. K. and Nachbauer, W. (1993). Effects of arch height of the foot on angular motion of the lower extremities in running. *J Biomech*, **26**, 909–916.

Nigg, B. M., Bahlsen, H. A., Luethi, S. M. and Stokes, S. (1987). The influence of running velocity and midsole hardness on external impact forces in heel-toe running. *J Biomech*, **20**, 951–959.

Pandy, M. G. and Berme, N. (1988). Synthesis of human walking: a planar model for single support. *J Biomech*, **21**, 1053–1060.

Pandy, M. G. and Berme, N. (1989). Quantitative assessment of gait determinants during single stance via a three-dimensional model — Part 1. Normal gait. *J Biomech*, **22**, 717–724.

Piazza, S. J. and Delp, S. L. (1996). The influence of muscles on knee flexion during the swing phase of gait. *J Biomech*, **29**, 723–733.

Raasch, C. C., Zajac, F. E., Ma, B. and Levine, W. S. (1997). Muscle coordination of maximum-speed pedaling. *J Biomech*, **30**, 595–602.

Reinschmidt, C., van den Bogert, A. J., Nigg, B. M., Lundberg, A. and Murphy, N. (1997). Effect of skin movement on the analysis of skeletal knee joint motion during running. *J Biomech*, **30**, 729–732.

Sandelin, J. and Santavirta, S. (1991). Occurrence and epidemiology of sports injuries in Finland. *Ann Chir Gynaecol*, **80**, 95–99.

Schutte, L. M., Rodgers, M. M., Zajac, F. E. and Glaser, R. M. (1993). Improving the efficacy of electrical stimulation-induced cycle ergometry: an analysis based on dynamic musculoskeletal model. *IEEE Trans Rehabil Eng*, **1**, 109–125.

Soderkvist, I. and Wedin, P. A. (1993). Determining the movements of the skeleton using well-configured markers. *J Biomech*, **26**, 1473–1477.

Soest, A. J. van and Bobbert, M. F. (1993). The contribution of muscle properties in the control of explosive movements. *Biol Cybern*, **69**, 195–204.

Stacoff, A., Denoth, X. K. and Stuessi, E. (1988). Running injuries and shoe construction: some possible relationships. *Int J Sport Biomech*, **4**, 342–357.

Van der Helm, F. C. and Veenbaas, R. (1991). Modelling the mechanical effect of muscles with large attachment sites: application to the shoulder mechanism. *J Biomech*, **24**, 1151–1163.

Van Mechelen, W. (1992). Running injuries. A review of the epidemiological literature. *Sports Med*, **14**, 320–335.

Winters, J. M. and Stark, L. (1988). Estimated mechanical properties of synergistic muscles involved in movements of a variety of human joints. *J Biomech*, **21**, 1027–1041.

Wright, I. C., Neptune, R. R., Bogert, A. J. van den and Nigg, B. M. (1998). Passive regulation of impact forces in heel-toe running. *Clin Biomech*, **13**, 521–531.

Wright, I. C., Neptune, R. R., Bogert, A. J. van den and Nigg, B. M. (1999). Validation of a 3D model for the simulation of ankle sprains. *J Biomech Eng*, Accepted.

Wright, I. C., Neptune, R. R., Bogert, A. J. van den and Nigg, B. M. (2000). The effects of ankle compliance and flexibility on ankle sprains. *Med Sci Sports Exerc*, **32**, 260–265.

Yamaguchi, G. T. and Zajac, F. E. (1990). Restoring unassisted natural gait to paraplegics via functional neuromuscular stimulation: a computer simulation study. *IEEE Trans Biomed Eng*, **37**, 886–902.